Advances in Nano Research, *Vol. 13, No.5 (2022) 417-426*
https://doi.org/10.12989/anr.2022.13.5.417

Coating gold nanoparticles to a glass substrate by spin-coat method as a surface-enhanced raman spectroscopy (SERS) plasmonic sensor to detect molecular vibrations of bisphenol-a (BPA)

Vahid Eskandari, Amin Hadi* and Hossein Sahbafar

Cellular and Molecular Research Center, *Yasuj University of Medical Sciences*, *Yasuj*, *Iran*

(*Received March 23, 2021, Revised April 17, 2022, Accepted June 7, 2022*)

Abstract. Bisphenol A (BPA) is one of the chemicals used in monomer epoxy resins and polycarbonate plastics. The surface-enhanced Raman spectroscopy (SERS) method is precise for identifying biological materials and chemicals at considerably low concentrations. In the present article, the substrates coated with gold nanoparticles have been studied to identify BPA and control the diseases caused by this chemical. Gold nanoparticles were made by a simple chemical method and by applying gold salt and trisodium citrate dihydrate reductant and were coated on glass substrates by a spin-coat approach. Finally, using these SERS substrates as plasmonic sensors and Raman spectroscopy, the Raman signal enhancement of molecular vibrations of BPA was investigated. Then, the molecular vibrations of BPA in some consumer goods were identified by applying SERS substrates as plasmonic sensors and Raman spectroscopy. The fabricated gold nanoparticles are spherical and quasi-spherical nanoparticles that confirm the formation of gold nanoparticles by observing the plasmon resonance peak at 517 nm. Active SERS substrates have been coated with nanoparticles, which improve the Raman signal. The enhancement of the Raman signal is due to the resonance of the surface plasmons of the nanoparticles. Active SERS substrates, gold nanoparticles deposited on a glass substrate, were fabricated for the detection of BPA; a detection limit of 10-9 M and a relative standard deviation (RSD) equal to 4.17% were obtained for ten repeated measurements in the concentration of 10-9 M. Hence, the Raman results indicate that the active SERS substrates, gold nanoparticles for the detection of BPA along with the developed methods, show promising results for SERS-based studies and can lead to the development of microsensors. In Raman spectroscopy, SERS active substrate coated with gold nanoparticles are of interest, which is larger than gold particles due to the resonance of the surface plasmons of gold nanoparticles and the scattering of light from gold particles since the Raman signal amplifies the molecular vibrations of BPA. By decreasing the concentration of BPA deposited on the active SERS substrates, the Raman signal is also weakened due to the reduction of molecular vibrations. By increasing the surface roughness of the active SERS substrates, the Raman signal can be enhanced due to increased light scattering from rough centers, which are the same as the larger particles created throughout the deposition by the spin-coat method, and as a result, they enhance the signal by increasing the scattering of light. Then, the molecular vibrations of BPA were identified in some consumer goods by SERS substrates as plasmonic sensors and Raman spectroscopy.

Keywords: bisphenol-a molecule (BPA); gold nanoparticles; plasmonic sensor; spin-coat method; surface-enhanced raman spectroscopy (SERS)

1. Introduction

Bisphenol A (BPA) is a chemical compound with the formula of $(CH_3)_2C(C_6H_4OH)_2$. BPA is one of the raw materials for producing plastics, the inner coating of many types of food and beverage cans, some polycarbonates and epoxy resins, as well as some polysulfones (Ntsendwana *et al*. 2012, Preethi *et al*. 2014, Rogers *et al*. 2013, Xiaowei Yu *et al*. 2013). Some researchers have indicated that BPA can permeate foods or beverages made from BPA containers. Getting exposed to BPA can potentially affect the brain, prostate gland, and other organs (Alonso-Magdalena *et al*. 2016, Le *et al*. 2008, Maragou *et al*. 2008). BPA is one of the Endocrine-disrupting chemicals (EDCs). These substances are a large group of natural and synthetic agents that interfere with the natural functioning of the endocrine system. These chemical compounds include environmental estrogens (xenoestrogens) such as phytoestrogens and human-made chemicals. These xenoestrogen compounds are diverse groups that bind to estrogen receptors and mimic the related actions of this hormone and probably have adverse effects on human health. These substances are associated with human health issues, including sperm quality, fertility, abnormalities in reproductive organs, premature puberty, nervous system function, immune system function, cancer, respiratory problems, metabolic problems, obesity, heart health, growth problems, disability, etc. (O'Sullivan 2017, O'Reilly *et al*. 2012, Preethi *et al*. 2014, Pupo *et al*. 2012). Therefore, the high accuracy detection of BPA in materials is of great importance. Various techniques such as High-Performance Liquid Chromatography (HPLC), Tandem Mass Spectrometry (TMS) (MS/MS), Gas Chromatography-Mass Spectrometry (GC-MS), Enzyme-linked Immune Sorbent Assay (ELISA), and Surface-enhanced Raman Spectroscopy (SERS) are

*Corresponding author, Ph.D.,
E-mail: amin.hadi@yums.ac.ir

ISSN: 2287-237X (Print), 2287-2388 (Online)

employed to detect BPA (Eskandari *et al*. 2022, Fan *et al*. 2012, Wang *et al*. 2012, 2013). Nanotechnology is the technology, science, and engineering that is conducted, researched, investigated, and experimented at the nanoscale (Adeli *et al*. 2017, Barati *et al*. 2020a, b, Dehshahri *et al*. 2020, Emadi *et al*. 2021, Eskandari and Hadi, 2020, Eskandari *et al*. 2022, Farajpour *et al*. 2014, Hadi *et al*. 2018a, b, 2019, Rohani Rad and Farajpour 2019, She *et al*. 2021). The SERS is a surface-sensitive technique that enhances Raman scattering by molecules adsorbed on rough metal surfaces or nanostructures (Eskandari *et al*. 2022). The SERS method is more sensitive than the other mentioned techniques (Ankamwar and Sur 2020, Madzharova *et al*. 2017). Raman spectroscopy is an appropriate method to identify the composition of various materials, including biological samples and chemicals, however, the Raman signals of biological samples and chemicals are not significant, especially at low concentrations (Su *et al*. 2019, Wang *et al*. 2019). In the SERS method, the Raman signal is improved due to the interaction between the surface plasmons of the metal and samples by placing different biological and chemical samples or physically adsorbing them on the surface containing metal nanoparticles. Thus, SERS can be used to detect biological and chemical samples (Zhou *et al*. 2014). Nowadays, layers composed of noble metal nanoparticles such as gold and silver have been considered due to the resonance of surface plasmons and optical properties. The light emission on noble metal nanoparticles causes oscillations of its conduction electrons to increase the energy density of electric fields or the irradiated light that is applied in biological sensors (Krasteva *et al*. 2002, Shrivastava and Dash 2010), solar cells (Wu *et al*. 2012), and SERS (McLellan *et al*. 2007). Due to the extraordinary optical properties of these nanoparticles, various methods such as lithography by electron beam (Berkovitch *et al*. 2010, Lucas *et al*. 2008) have been proposed for the fabrication of layers consisting of metal nanoparticles (Xiuping Yu *et al*. 2011). Lithography by electron beam method requires complex and expensive equipment and is employed to produce small-scale samples. On the contrary, the electrochemical deposition method is simple to produce large-scale samples (Liang *et al*. 2010, Zhang *et al*. 2011). Raman scattering results from the inelastic scattering of light from matter, and very detailed information about the structure of a molecule can be obtained using this effect. The IR spectroscopy complicates the detection of biological and chemical samples due to the active molecular vibrations of water, and also, the sensitivity of its detectors is low. Electron- and ion-based spectrometers also require a high vacuum, hence, Raman spectroscopy allows the study of molecules under normal conditions and can also be used to investigate catalytic processes and those occurring in the metal-electrolyte interface (Cyrankiewicz *et al*. 2007). The signal related to Raman scattering is inherently weak and makes the detection challenging (Duan *et al*. 2016). The use of metal nanostructures is one of the methods to enhance the Raman signal, this selective and sensitive technique, called SERS, can enhance the scattering signal due to the resonance of surface plasmons. The enhancement of Raman scattering of molecules adsorbed on metal structures is of the results of applying this method (Wang and Fang 2006). This phenomenon was first observed in 1974 for electrochemically cultured pyridine molecules adsorbed on the surface of silver electrodes. The enhanced Raman signal was observed only after the silver electrode was placed in the oxidation-reduction or activation cycle and did not show any enhanced signal for a smooth surface. First, signal enhancement was described based on an increase in the number of studied molecules due to the increase in the surface area that has been roughened, however, the enhancement of the Raman signal must have had a reason other than the increase in surface area. In 1977, an enhanced Raman signal was attributed to the molecule's interaction with the surface of the roughened metal (Jing and Fang, 2007). Metals such as gold, silver, copper, and platinum have been employed to observe this phenomenon. Metals' properties, including type, shape, size, and arrangement, affect the Raman scattering of the studied molecule. Among the various metals, silver and gold have received more attention thanks to their plasmonic resonance in the visible and infrared region, higher stability, and easy fabrication methods to detect biological samples and chemicals (Cañamares *et al*. 2008).

In the present article, gold nanoparticles were coated by the spin-coat method on the glass substrates with high mechanical adhesion, fast, and low cost at room temperature to be applied as plasmonic sensors of active SERS substrates detecting molecular vibrations of BPA at low concentrations. Then, the molecular vibrations of BPA were detected in some consumer goods by active SERS substrates as plasmonic sensors and Raman spectroscopy.

2. Materials and methods

2.1 Chemicals

The materials used in the present study include $HAuCl_4.3H_2O$ gold salt (chloroauric *acid trihydrate*) with a molar mass of 393.833 g/mol and a purity higher than 99.95%, trisodium citrate dihydrate with a molar mass of 294.1 g/mol and a purity higher than 99%, Bisphenol A (BPA) with a molar mass of 228.29 g/mol and a purity higher than 99.95%, and (3-Aminopropyl)triethoxysilane (APTES) prepared by Sigma-Aldrich, glass slices as substrates with the dimensions of 2.5cm×7.5cm, Acetone with a molar mass of 58.09 g/mol and a purity higher than 99.95%, and ethanol with a molar mass of 46.069 g/mol and a purity higher than 99.95% prepared by Merck & Co.

2.2 Fabrication methods of active SERS substrates as plasmonic sensors

The glasses were cut with the dimensions of 2cm×2cm to be used as substrates. After washing with soap, water, acetone, and ethanol, the samples were heated in a furnace at 400 °C for 30 minutes to remove contaminants of organic materials from the glass surface so that some hydrophilic surfaces were prepared to coat the glass with gold nano-

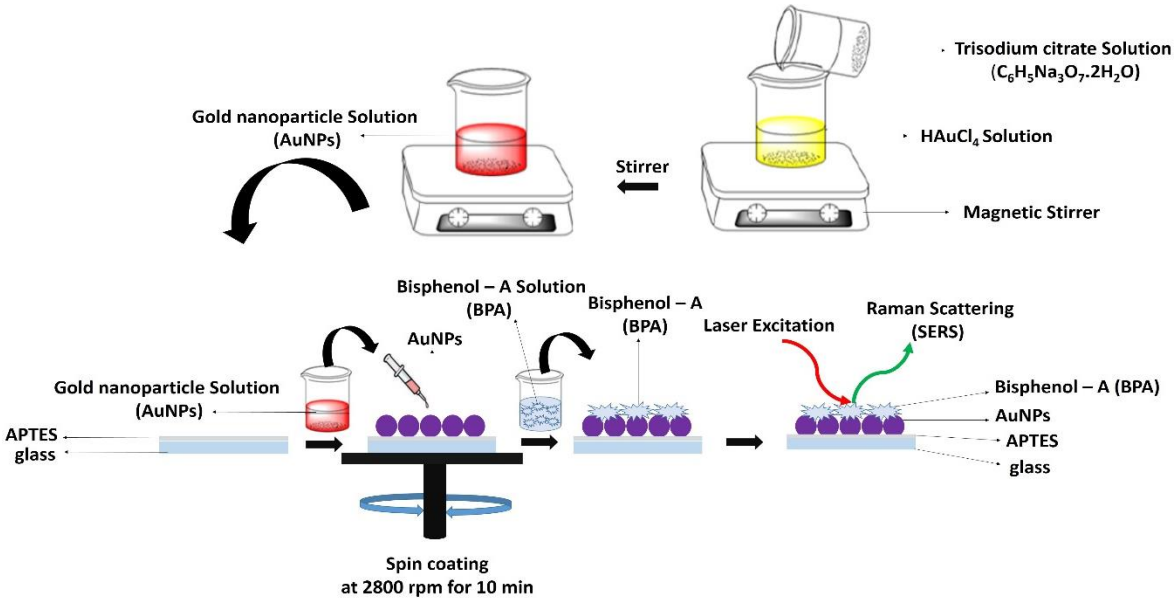

Fig. 1 The schematic preparation of colloidal gold solution by chemical method and fabrication of active SERS substrates as plasmonic sensors through depositing gold nanoparticles inside gold colloidal solution on glass substrates under 2500 rpm for 10 minutes by the spin-coat method and dropping different concentrations of BPA molecule on active SERS substrates as plasmonic sensors to detect these molecules

particles. These glasses were then placed in a piranha solution (H_2O_2/H_2SO_4 = 3:7 v/v) at 80 °C. After 30 minutes, the glasses were washed with DI water and immediately transferred to the boiling solution ($H_2O_2/NH_3/H_2O$ = 1:1:5 v/v/v). After 30 minutes, they were washed with DI water, and the activated surface of the glasses was immersed in a 1% APTES solution of ethanol for 24 hours. The functionalized surface of the glasses was washed frequently with ethanol to remove additional reagents from the surface and finally dried for 1 hour at 110 °C (Creedon, 2018). Then, for producing gold nanoparticles, 1 ml of 38.8 mM solution of trisodium citrate dihydrate ($NaC_6H_5O_7.H_2O$) was added to 20 ml of 1 mM solution of boiling and stirring gold salt ($HAuCl_4$), the final colloid of amethyst color contains gold nanoparticles (Iqbal *et al*. 2016). In the next step, APTES and gold nanoparticles were deposited inside the gold colloidal solution on glass substrates using the spin-coat method. For this purpose, glass substrates were placed in a spin-coat machine, then 10 µl of APTES was dispersed on glass substrates and deposited for 2 minutes at 2500 rpm, and then 100 µl of this colloidal gold solution was dispersed on glass substrates, and the deposition was performed at 2500 rpm for 10 minutes, and the gold nanoparticle coated substrates were dried at laboratory temperature. In order to detect BPA molecules, the concentrations 10^{-1}, 10^{-2}, 10^{-3}, 10^{-4}, 10^{-5}, 10^{-6}, 10^{-7}, 10^{-8}, and 10^{-9} M of BPA with DI solution were prepared separately by a dropper, 10 µl of each of the prepared concentrations was placed on active SERS substrates as plasmonic sensors, and after being dried in the presence of air, Raman spectra of BPA deposited on glass, and surface-enhanced Raman spectra of active SERS substrates were measured and analyzed as plasmonic sensors, and then molecular vibrations of BPA in some consumer goods were detected by SERS substrates as plasmonic sensors and Raman spectroscopy.

2.3 Characterization

The UV-Vis spectroscopy of colloidal solution of gold nanoparticles and active SERS substrates was performed as plasmonic sensors by the Perkin-Elmer Lambda 25 device at room temperature. Field Emission Scanning Electron Microscope (FESEM) images were analyzed by Hitach S4160, and Atomic Force Microscope (AFM) images were analyzed using the device manufactured by an Iranian company named Nanotechnology System Corporation (NATSYCO). Confocal Raman Spectromicroscopy Lab Ram HR made by Horiba company with laser radiation of a wavelength of 633 nm and output power of 17 mW was applied to measure the Raman spectra and SERS spectra of the samples.

3. Results and discussion

3.1 Biosensor characterization

Fig. 2(a) shows the absorption spectra of gold nanoparticles made chemically with the tri-sodium citrate dihydrate reductant. The emergence of a plasmonic resonance peak at 517 nm confirms the formation of gold nanoparticles (Ngumbi *et al*. 2018), and observation of an absorption peak in the absorption spectra of gold nanoparticles indicates the spherical or quasi-spherical shape of the nanoparticles (Baytekin *et al*. 2015). Fig. 2(b) demonstrates the extinction spectra of gold nanoparticles coated on active SERS substrate as plasmonic sensors. As shown in Fig. 2(a), the deposition of gold nanoparticles on glass substrates and the emergence of a plasmonic resonance peak at 553 nm confirmed the formation of gold nanoparticles on glass substrates. By changing the medium

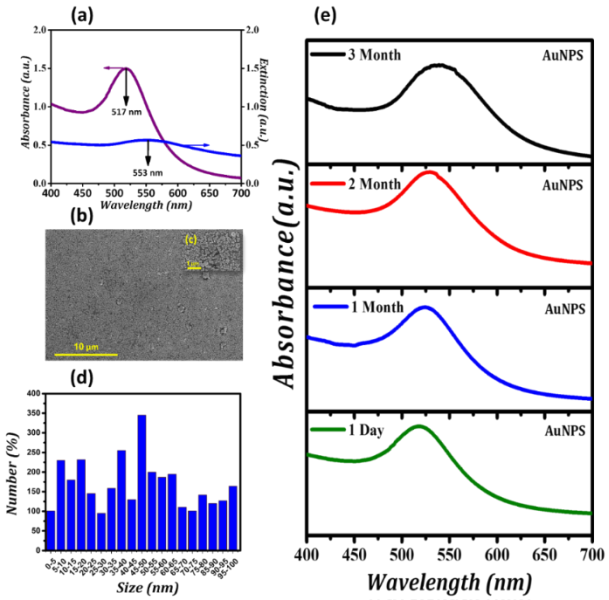

Fig. 2 (a) Absorption spectra of gold nanoparticles made by the chemical method with maximum absorption at the wavelength of 517 nm and extinction spectra of active SERS substrates of gold nanoparticles as plasmonic sensors with maximum extinction at the wavelength of 553 nm; (b) FE-SEM image related to active SERS substrates as plasmonic sensors in scale bar of 10 microns, which was made in the amount of 100 microliters of gold nanoparticles in 10 minutes by spin-coat method; (c) FE-SEM image of the active SERS substrates as plasmonic sensors at a scale bar of 1 µm; (d) Size distribution diagram of gold nanoparticles in the FE-SEM image of active SERS substrates as plasmonic sensors at a scale bar of 10 µm measured by Digimizer software (version 4.2); (e) UV-Vis spectroscopy of gold nanoparticles made by the chemical method with trisodium citrate dihydrate to evaluate the stability of gold nanoparticles (for three months).

containing these particles that change from water to glass and air, the displacement occurs at the wavelength of the plasmonic peak, and its height decreases, and the width of the peaks increases since the position of the plasmonic peak depends on the refractive index of the medium (Bohren and Huffman 2008). According to Fig. 2(a), in contrast to the stable colloidal solution, gold nanoparticles are dispersed in an aqueous solution and at certain distances from each other. By depositing gold nanoparticles on glass substrates during drying, the particles are placed next to each other, and agglomerates consisting of several nanoparticles are formed on the substrates so that these agglomerates can be considered as larger particles that lead to an increase in the spectrum width (Bohren & Huffman, 2008). The decrease in peak intensity is also due to light scattering from agglomerated particles (Bohren & Huffman, 2008). The occurrence of the field of extinction spectra (absorption spectra + scattering spectra) of active SERS substrates as plasmonic sensors at higher amounts compared to absorption spectra is due to the reflection and scattering of light from the glass surface. Fig. 2(b) indicates the FE-SEM image of the active SERS substrates as a plasmonic sensor at a scale of 10 microns. In the sample shown in Fig. 2)b), the surface of the glass substrate has been coated with nanoparticles and larger particles. Smaller particles of darker colors are observed in the background of the images, which are approximately 50 nm in size. The coating involving gold nanoparticles has coated the glass surface relatively homogeneously and uniformly. Fig. 2(c) indicates the FE-SEM image of the active SERS substrates as a plasmonic sensor at a scale bar of 1 µm. Larger particles appear brighter and whiter. Smaller gold nanoparticles lead to significant near electric fields around themselves that result from the resonance of surface plasmons of gold, and in the case that BPA chemical samples are placed in these positions, they will also be exposed to near electric fields. Larger particles have negligible near electric fields, and the light emitted on them is scattered from their surface or amplifies the far electric field (Ding *et al*. 2017). Therefore, with increasing the deposition time for 10 minutes, due to the formation of larger particles, the effect of scattering from the surface of the larger particle is more significant than the effect of the near field.

In Fig. 2(d), the size distribution of gold nanoparticles has been measured using Digimizer software (version 4.2), which shows that their sizes range from 5 nm to 100 nm, and the number of particles with the size of 45 nm and 50 nm is more than other nanoparticles. In Fig. 2(e), UV-Vis spectroscopy has been evaluated for reaching the stability of gold nanoparticles in the presence of the trisodium citrate dihydrate; after three months, the gold nanoparticles were prepared with the trisodium citrate dihydrate showed an excellent rate of stability.

3.2 AFM ımages of gold nanoparticles coated on active SERS glass substrates as plasmonic sensors

Figs. (3a) and (3b) indicate the two-dimensional and three-dimensional AFM images of active SERS substrates as plasmonic sensors of gold nanoparticles coated on a glass substrate, respectively. Fig. 3(c) shows the roughness plot of the surface of active SERS substrates of gold nanoparticles coated on the glass substrate, and the characteristics of surface roughness were calculated by Image Plus software (version 2.9) by drawing a green line from the diameter of Fig. 3(b). Roughness average (Ram), the average maximum height of the roughness (Rtm), and average maximum roughness valley depth were calculated to be 28.2 nm (0.0282 µm), 129.6 nm (0.1296 µm), and 104.1 nm (01041 µm). The surface roughness created by active SERS substrates of gold nanoparticles coated on the glass substrate can be the center for light scattering and amplify the Raman signal (Baytekin *et al*. 2015).

3.3 Raman spectra and detecting BPA using gold nanoparticles coated on active SERS glass substrates as plasmonic sensors

Raman spectra of glass substrates (brown curve), Raman spectra of gold nanoparticles coated on glass substrates (red curve), Raman spectra of BPA of concentration of 10^{-1} M deposited on the glass substrate (blue curve), and SERS spectra of BPA molecule of a concentration of 10^{-1} M deposited on active SERS substrates, gold nanoparticles

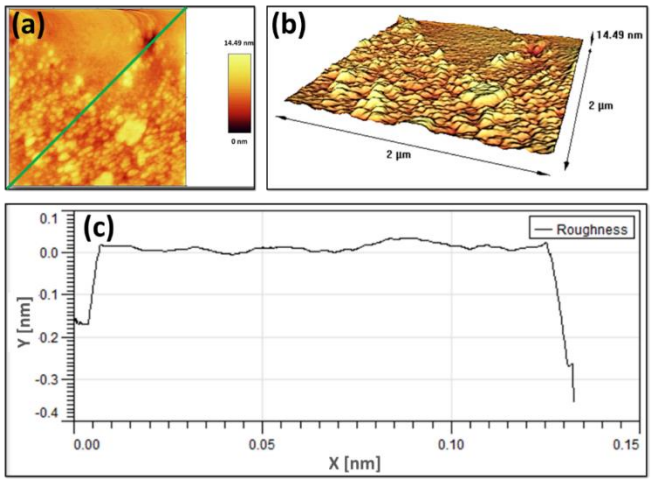

Fig. 3 (a) Two-dimensional AFM images; (b) three-dimensional AFM images; and (c) roughness plot of active SERS substrates of gold nanoparticles coated on the glass substrate

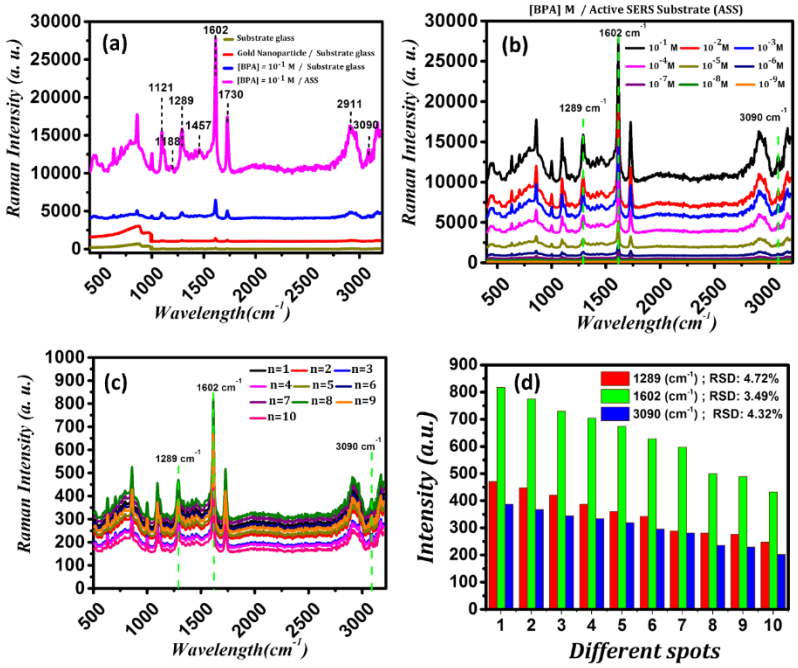

Fig. 4 (a) Raman spectra of the glass substrate (brown curve), Raman spectra of gold nanoparticles coated on glass substrates (red curve), Raman spectra of BPA of concentration of 10^{-1} M deposited on glass substrates (blue curve), SERS spectra of BPA of concentration of 10^{-1} deposited on active SERS substrates of gold nanoparticles coated on glass substrates (pink curve); (b) SERS spectra of BPA of concentrations of 10^{-1} (black curve), 10^{-2} (red curve), 10^{-3} (blue curve), 10^{-4} (pink curve), 10^{-5} (Brown curve), 10^{-6} (blue-dark curve), 10^{-7} (purple curve), 10^{-8} (green curve) and 10^{-9} (orange curve) molar of gold nanoparticles coated on glass substrates; (c) SERS spectra of ten separate points from BPA of concentration of 10^{-9} M at a volume of 10 µL added on active SERS substrates of gold nanoparticles coated on glass substrates. Diagram of changes in ten continuous experiments of BPA with a concentration of 10^{-9} M; the value of RSD has been calculated to be 4.72%, 3.49%, and 4.32% for the peaks at wavelengths of 1289 cm^{-1}, 1602 cm^{-1}, and 3090 cm^{-1}, respectively; (d) the RSD variations are indicated as a bar chart and calculated to be 4.79% (red diagram), 3.49% (green diagram), and 4.32% (blue diagram) for wavelengths of 1289 cm^{-1}, 1602 cm^{-1}, and 3090 cm^{-1}, respectively.

coated on glass substrates (pink curve) are observed in Fig. 4(a). In Raman spectra of BPA deposited on the glass substrate (blue curve), no molecular vibrations of BPA are observed. Hence, it is practically impossible to detect these chemicals even with a concentration of 10^{-1} M and using Raman spectroscopy. By depositing BPA of a concentration of 10^{-1} M on the active SERS substrates, gold nanoparticles coated on glass substrates, and molecular vibrations of BPA emerge. Molecular vibrations of BPA (Lee *et al*. 2000, Rodriguez-Gonzalez *et al*. 2013) are indicated as dashed

lines on BPA spectra in Fig. 4(a). In the case of BPA molecule deposited on active SERS substrates, gold nanoparticles coated on glass substrates, flexural vibrations of C-H, flexural vibrations of C-H, tensile vibrations of C-O, flexural vibrations of C-H, tensile vibrations of the phenyl ring, tensile vibrations of C-O, tensile vibrations of benzene rings, and tensile vibrations of phenyl-hydrogen ring emerge at 1121 cm^{-1}, 1188 cm^{-1}, 1289 cm^{-1}, 1457 cm^{-1}, 1602 cm^{-1}, 1730 cm^{-1}, 2911 cm^{-1}, and 3090 cm^{-1}, respectively. The enhancement of the Raman signal is due to the use of active SERS substrates of gold nanoparticles coated on glass substrates because of light scattering from rough points. Larger gold particles observed in Fig. 2(b) enhance the Raman signal by scattering incident laser light and reaching the scattered light to BPA. Another reason for the enhancement of the Raman signal is the resonance of surface plasmons of smaller gold particles or the strong electric fields around these nanoparticles. The gold nanoparticles demonstrated in Fig. 2(b) act similar to optical lenses and focus incident laser light around themselves. Therefore, the intensity of the electric field near the nanoparticles increases, and BPA experiences a strong electric field and becomes more polarized by depositing BPA around the nanoparticles, resulting in amplified molecular vibrations and more intensive signals (Chen *et al*. 2015, Granger *et al*. 2016).

Fig. 4(b) shows the SERS spectra of BPA with concentrations of 10^{-1} (black curve), 10^{-2} (red curve), 10^{-3} (blue curve), 10^{-4} (pink curve), 10^{-5} (brown curve), 10^{-6} (dark blue curve), 10^{-7} (purple curve), 10^{-8} (green curve), and 10^{-9} (orange curve) molar of gold nanoparticles coated on glass substrates. As the BPA concentration decreases, the intensity of the peaks of its molecular vibrations is reduced due to the decrease in the number of BPA molecules, resulting in a reduction of the number of molecular vibrations so that BPA vibrations are not readily visible in the concentrations lower than 10^{-9} M. Therefore, active SERS substrates of gold nanoparticles coated on glass substrates can detect the BPA of concentrations up to 10^{-9} M. Then, in order to achieve the repeatability in fabricating the active SERS substrates of gold nanoparticles coated on glass substrates, ten continuous experiments were performed for a concentration of 10^{-9} M of BPA during one day. Fig. 4(c) shows the SERS spectra of ten separate points of BPA at a concentration of 10^{-9} M and a volume of 10 µL deposited on active SERS substrates of gold nanoparticles coated on glass substrates. It is evident that all SERS spectra of BPA are properly fitted at concentrations of 10^{-9} M, and no change in the displacement and characteristics of the spectra is observed. Relative standard deviation (RSD) was calculated by Eq. (1) for the peaks at wavelengths of 1289 cm^{-1}, 1602 cm^{-1}, and 3090 cm^{-1} to evaluate the repeatability of fabricating active SERS substrates of gold nanoparticles coated on glass substrates at a concentration of 10^{-9} M of BPA (Parsons *et al*. 2009).

$$RSD = \frac{\sqrt{\sum_{i=1}^{n} \frac{(I_i - I)^2}{n-1}}}{I} \quad (1)$$

where n = 10 is the number of tested Raman spectra, I_i implies the intensity of the Raman signal at each specified peak, and I denote the average intensity of the Raman signal of the specified peaks. Fig. 4(c) presents the diagram of the changes of ten continuous experiments of BPA at a concentration of 10^{-9} M for peaks at wavelengths of 1289 cm^{-1}, 1602 cm^{-1}, and 3090 cm^{-1} with RSD values of 4.72%, 3.49%, and 4.32%, respectively. In Fig. 4(d), the calculation changes of RSD have been calculated for the wavelengths of 1289 cm^{-1}, 1602 cm^{-1}, and 3090 cm^{-1} to be 4.72% (red diagram), 3.49% (green diagram), and 4.32% (blue diagram) and specified as a bar chart. The RSD obtained in this experiment was 4.15% on average, which statistically indicates the satisfactory performance of the method applied to determine BPA concentration. Other methods that have been used to determine the concentration of BPA in different samples include gas and liquid chromatography with mass detectors, however, low detection limits have been achieved for them, numerous sample preparations are required, and also the cost and time of sample preparation and analysis are high (Fan *et al*. 2012, Q. Wang *et al*. 2012, Xiaowei Yu *et al*. 2013).

3.4 Calibration curve of ıntensity changes, raman spectra and detection of BPA using gold nanoparticles coated on active SERS glass substrates as plasmonic sensors

Fig. 5(a) shows the intensity diagram of SERS spectra of BPA molecule adsorbed on active SERS substrates of gold nanoparticles coated on glass substrates relative to variations in 10^{-1}, 10^{-2}, 10^{-3}, 10^{-4}, 10^{-5}, 10^{-6}, 10^{-7}, 10^{-8}, and 10^{-9} concentrations of BPA molecules in molar for peaks at a wavelength of 1289 cm^{-1} (black curve), 1602 cm^{-1} (red curve), and 3090 cm^{-1} (blue curve). Fig. 5(b) is the calibration curve that indicates the changes in the intensity of the SERS signal and tensile vibrations of C-O at a wavelength of 1289 cm^{-1} in terms of logarithmic changes in the concentration of BPA molecule, C, which follows Eq. (2) by performing the fitting operations.

$$I = 291.275\,C^2 + 4815.409\,C + 20089.791 \quad (R^2 = 0.99267) \quad (2)$$

where the regression coefficient (R^2) is equal to 0.99267.

Fig. 5(c) indicates the SERS spectra shown in Fig. 5(b) and SERS spectra of BPA with concentrations of 10^{-1} (black curve), 10^{-2} (red curve), 10^{-3} (blue curve), 10^{-4} (pink curve), 10^{-5} (brown curve), 10^{-6} (dark blue curve), 10^{-7} (purple curve), 10^{-8} (green curve), and 10^{-9} (orange curve) in molar scales deposited on the active SERS substrate shown in the range of 1260-1320 cm^{-1}. By applying this diagram and observing the peak intensity of molecular vibrations, the tensile vibrations of C-O at a wavelength of 1289 cm^{-1} for an uncertain amount of BPA molecules, its concentration can be obtained. Fig. 5(d) is the calibration curve that indicates the changes in the intensity of the SERS signal and tensile vibrations of the phenyl ring at a wavelength of 1602 cm^{-1} in terms of logarithmic changes in the concentration of BPA molecule, C, which follows Equation (3) by performing the fitting operations.

$$I = 505.196\,C^2 + 8385.303\,C + 35015.833 \quad (R^2 = 0.99349) \quad (3)$$

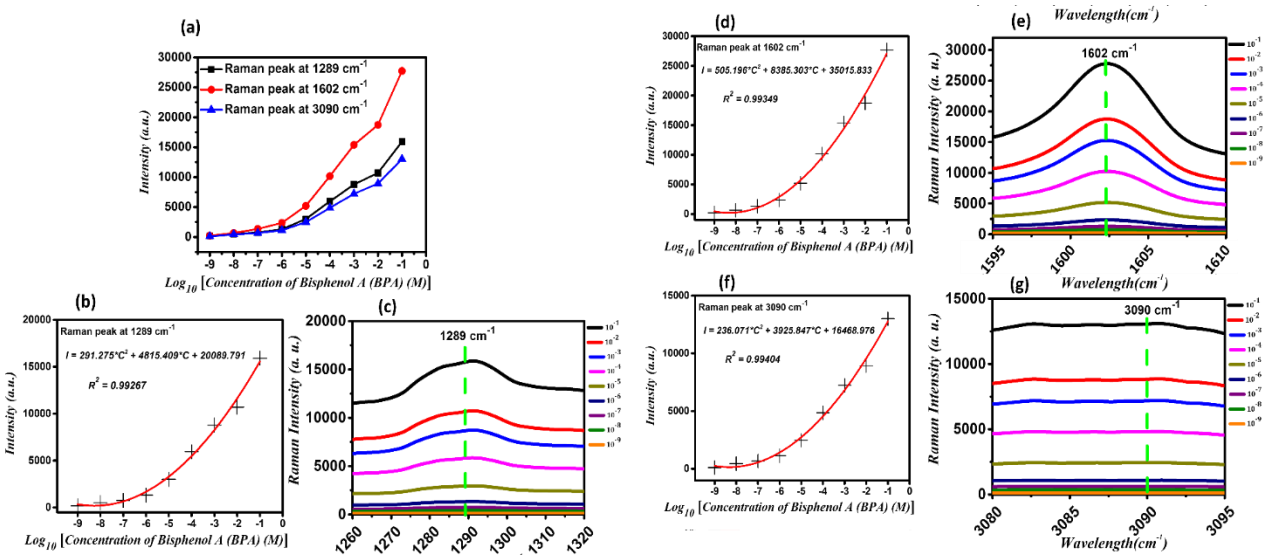

Fig. 5 (a) The intensity diagram of SERS spectra of BPA molecule adsorbed on active SERS substrate of gold nanoparticles coated on glass substrates relative to variations in 10^{-1}, 10^{-2}, 10^{-3}, 10^{-4}, 10^{-5}, 10^{-6}, 10^{-7}, 10^{-8}, and 10^{-9} concentrations of BPA molecules in molar for peaks at wavelength of 1289 cm^{-1} (black curve), 1602 cm^{-1} (red curve), and 3090 cm^{-1} (blue curve); (b) The calibration curve that indicates the changes in I of SERS signal related to molecular vibrations, tensile vibrations of C-O at wavelength of 1289 cm^{-1} in terms of logarithmic changes in the concentration of BPA molecule, C, of active SERS substrate of gold nanoparticles coated on glass substrates extracted from Fig. (4b); (c) The SERS spectra shown in Fig. (5b) and SERS spectra of BPA with concentrations of 10^{-1} (black curve), 10^{-2} (red curve), 10^{-3} (blue curve), 10^{-4} (pink curve), 10^{-5} (brown curve), 10^{-6} (dark blue curve), 10^{-7} (purple curve), 10^{-8} (green curve), and 10^{-9} (orange curve) in molar scales deposited on the active SERS substrate shown in the range of 1260-1320 cm^{-1}. By applying this diagram and observing the peak intensity of molecular vibrations, the tensile vibrations of C-O at wavelength 1289 cm^{-1} for an uncertain amount of BPA molecules, its concentration can be obtained; (d) The calibration curve that indicates the changes in I of SERS signal related to molecular vibrations, tensile vibrations of phenyl ring at wavelength 1602 cm^{-1} in terms of logarithmic changes in the concentration of BPA molecule, C, of active SERS substrate of gold nanoparticles coated on glass substrates extracted from Fig. (4b); (e) The SERS spectra shown in Fig. (5d) and SERS spectra of BPA with concentrations of 10^{-1} (black curve), 10^{-2} (red curve), 10^{-3} (blue curve), 10^{-4} (pink curve), 10^{-5} (brown curve), 10^{-6} (dark blue curve), 10^{-7} (purple curve), 10^{-8} (green curve), and 10^{-9} (orange curve) in molar scales deposited on the active SERS substrate shown only in the range of 1595-1610 cm^{-1}. By applying this diagram and observing the peak intensity of molecular vibrations, the tensile vibrations of C-O at a wavelength of 1602 cm^{-1} for an uncertain amount of BPA molecules, its concentration can be obtained; (f) The calibration curve that demonstrates the changes in I of SERS signal related to tensile vibrations of the phenyl-hydrogen ring at a wavelength of 3090 cm^{-1} in terms of logarithmic changes in the concentration of BPA molecule, C, of active SERS substrate of gold nanoparticles coated on glass substrates extracted from Fig. (4b); (g) The SERS spectra shown in Fig. (5f) and SERS spectra of BPA with concentrations of 10^{-1} (black curve), 10^{-2} (red curve), 10^{-3} (blue curve), 10^{-4} (pink curve), 10^{-5} (brown curve), 10^{-6} (dark blue curve), 10^{-7} (purple curve), 10^{-8} (green curve), and 10^{-9} (orange curve) in molar scales deposited on the active SERS substrate shown in the range of 3080-3095 cm^{-1}. By applying this diagram and observing the peak intensity of molecular vibrations, the tensile vibrations of the phenyl-hydrogen ring at a wavelength of 3090 cm^{-1} for an uncertain amount of BPA molecules, its concentration can be obtained.

where the regression coefficient (R^2) is equal to 0.99349.

Fig. 5(e) indicates the SERS spectra shown in Fig. 5(d) and SERS spectra of BPA with concentrations of 10^{-1} (black curve), 10^{-2} (red curve), 10^{-3} (blue curve), 10^{-4} (pink curve), 10^{-5} (brown curve), 10^{-6} (dark blue curve), 10^{-7} (purple curve), 10^{-8} (green curve), and 10^{-9} (orange curve) in molar scales deposited on the active SERS substrate shown in the range of 1595-1610 cm^{-1}. By applying this diagram and observing the peak intensity of molecular vibrations, the tensile vibrations of C-O at a wavelength of 1602 cm^{-1} for an uncertain amount of BPA molecules, its concentration can be obtained. Fig. 5(f) is the calibration curve that demonstrates the changes in the intensity of the SERS signal and tensile vibrations of the phenyl-hydrogen ring at a wavelength of 3090 cm^{-1} in terms of logarithmic changes in the concentration of BPA molecule, C, which follows Eq. (4) by performing the fitting operations.

$$I = 236.071\,C^2 + 3925.847\,C + 16468/976 \quad (R^2 = 0.99404) \tag{4}$$

where the regression coefficient (R^2) is equal to 0.99404.

Fig. 5(g) indicates the SERS spectra shown in Fig. 5(f) and SERS spectra of BPA with concentrations of 10^{-1} (black curve), 10^{-2} (red curve), 10^{-3} (blue curve), 10^{-4} (pink curve),

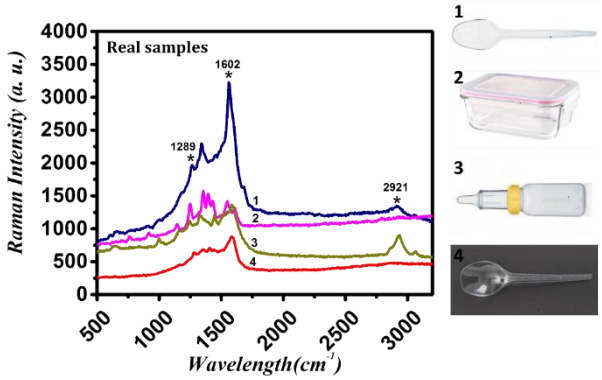

Fig. 6 Raman spectra and BPA detection using gold nanoparticles coated on active SERS glass substrates as plasmonic sensors in real samples of some consumer goods: 1) plastic spoon, 2) plastic container (for storing bread), 3) powdered milk bottles, and 4) transparent plastic spoons.

10^{-5} (brown curve), 10^{-6} (dark blue curve), 10^{-7} (purple curve), 10^{-8} (green curve), and 10^{-9} (orange curve) in molar scales deposited on the active SERS substrate shown in the range of 3080-3095 cm^{-1}. By applying this diagram and observing the peak intensity of molecular vibrations, the tensile vibrations of the phenyl-hydrogen ring at a wavelength of 3090 cm^{-1} for an uncertain amount of BPA molecules, its concentration can be obtained. Since the purpose of fabricating the plasmonic sensors of active SERS substrate is to detect very low concentrations of BPA molecules, the linearity of calibration curves of the low concentrations is of great importance and can be observed in the present study. By applying this diagram and observing the peak intensity of molecular vibrations of the molecule in Raman spectra, its concentration can be obtained.

3.5 Raman spectra and BPA detection using gold nanoparticles coated on active sers glass substrates as plasmonic sensors in real samples of some plastic consumer goods

In the following, real samples of some consumer goods were used to investigate the application of the fabricated sensor to detect BPA using gold nanoparticles coated on active SERS glass substrates as plasmonic sensors. Maragou *et al*. (2008) and Nerin *et al*. (2003) suggested that when the boiled water is added to powdered milk bottles, 2.4-14.3 mg/kg of BPA is added to the liquid. According to Fig. 6, some samples of plastic containers, including 1) plastic spoon, 2) plastic container (for storing bread), 3) powdered milk bottle, and 4) transparent plastic spoons, were used in the present study. Afterward, 500 ml of boiled water was prepared and poured separately on each of the samples, and 10 ml of water poured on each of the real samples was collected, and then SERS spectra were investigated for the detection of BPA by applying gold nanoparticles coated on active SERS glass substrates as plasmonic sensors in real samples of some consumer goods. As shown in Fig. 6, molecular vibrations of BPA emerge by placing 10 µL of water poured on each of the real samples collected on the active SERS substrate of gold nanoparticles coated on glass substrates. Molecular vibrations of BPA in four real samples are indicated in Fig. 6. For the BPA molecule in four real samples placed on the active SERS substrate of gold nanoparticles coated on glass substrates, tensile vibrations of C-O, the phenyl ring, and the benzene rings appear at 1289 cm^{-1}, 1602 cm^{-1}, and 2911 cm^{-1}, respectively. Therefore, the Raman results indicate that active SERS substrate of gold nanoparticles for detecting BPA in real samples of consumer goods by the developed methods show promising results for SERS-based studies and can lead to the development of microsensors.

4. Conclusions

The Raman signal can be enhanced by exposing the BPA molecule to the resonance of surface plasmons of metal nanoparticles such as gold and the scattering of light from large metal particles. Therefore, first, gold nanoparticles with an approximate size of 20 nm were produced using the chemical reduction method, and then the gold nanoparticles were deposited on glass substrates under 2800 rpm and at room temperature for 10 minutes using the spin-coat method, which is a simple, fast, and cheap technique. These substrates were applied as active SERS substrates for detecting the BPA molecule. The Raman signal of BPA is enhanced by placing BPA on active SERS substrates in all different samples and concentrations of BPA due to the resonance of surface plasmons of nanoparticles deposited on the glass surface by the spin-coat method. They receive incident laser light and concentrate it in a small area around themselves; the BPA molecule becomes more polarized, resulting in more intense vibrations by placing the BPA molecule in these areas and due to receiving a stronger electric field. Observing the plasmonic peak of the active SERS substrates of biological nanosensors of gold nanoparticles as an aqueous phase colloidal solution or deposited on the fabricated glass substrate at 517 nm and 553 nm, respectively, the deposition of gold nanoparticles on glass substrates was confirmed. By observing the FESEM images, the active SERS substrate of gold nanoparticles deposited on the glass substrate was confirmed. The roughness of the active SERS substrate of gold nanoparticles deposited on the glass substrate, resulting from the non-uniformity of the gold nanoparticles, leads to the scattering of light from points observed in the image of the electron microscope. The roughness observed in the AFM image for the active SERS substrate of gold nanoparticles deposited on the glass substrate assists in scattering light from rough points. The active SERS substrate of gold nanoparticles deposited on a glass substrate was fabricated to detect BPA molecules; the evaluation was performed for the detection limit of 10^{-9} M, and the RSD was calculated to be 4.15% for ten repeated measurements at a concentration of 10^{-9} M. Afterward, real samples of some consumer goods were used to investigate the application of the fabricated sensor to detect BPA using gold nanoparticles coated on active SERS glass substrates as plasmonic sensors. Therefore, the Raman results

obtained for active SERS substrates of gold nanoparticles deposited on a glass substrate for detecting the BPA molecule by developed methods show promising results for SERS-based studies and can lead to the development of microsensors. High detection speed, sensitivity, selectivity, repeatability, ease of use, and the rapid detection of low concentrations are the advantages of active SERS substrate of gold nanoparticles deposited on an introduced glass substrate; its fabrication is not expensive and can detect a variety of pathogens in food, biological materials, and chemicals

References

Adeli, M.M., Hadi, A., Hosseini, M. and Gorgani, H.H. (2017), "Torsional vibration of nano-cone based on nonlocal strain gradient elasticity theory", *Eur. Phys. J. Plus*, **132**(9), 393. https://doi.org/10.1140/epjp/i2017-11688-0.

Alonso-Magdalena, P., Rivera, F.J. and Guerrero-Bosagna, C. (2016), "Bisphenol-A and metabolic diseases: epigenetic, developmental and transgenerational basis", *Environ. Epigenet.*, **2**(3), dvw022. https://doi.org/10.1093/eep/dvw022.

Ankamwar, B. and Sur, U.K. (2020), "Copper micro/ nano-structures as effective SERS active substrates for pathogen detection", *Adv. Nano Res.*, **9**(2), 113-122. https://doi.org/10.12989/anr.2020.9.2.113.

Barati, A., Adeli, M.M. and Hadi, A. (2020a), "Static torsion of bi-directional functionally graded microtube based on the couple stress theory under magnetic field", *Int. J. Appl. Mech.*, **12**(2), 2050021. https://doi.org/10.1142/S1758825120500210.

Barati, A., Hadi, A., Nejad, M.Z. and Noroozi, R. (2020b), "On vibration of bi-directional functionally graded nanobeams under magnetic field", *Mech. Based Des. Struct.*, **50**(2), 468-485. https://doi.org/10.1080/15397734.2020.1719507.

Baytekin, H.T., Baytekin, B., Huda, S., Yavuz, Z. and Grzybowski, B.A. (2015), "Mechanochemical activation and patterning of an adhesive surface toward nanoparticle deposition", *J. Am. Chem. Soc.*, **137**(5), 1726-1729. https://doi.org/10.1021/ja507983x.

Berkovitch, N., Ginzburg, P. and Orenstein, M. (2010), "Concave plasmonic particles: broad-band geometrical tunability in the near-infrared", *Nano Lett.*, **10**(4), 1405-1408. https://doi.org/10.1021/nl100222k.

Bohren, C.F. and Huffman, D.R. (2008), *Absorption and Scattering of Light by Small Particles*, John Wiley & Sons.

Cañamares, M., Garcia-Ramos, J., Sanchez-Cortes, S., Castillejo, M. and Oujja, M. (2008), "Comparative SERS effectiveness of silver nanoparticles prepared by different methods: A study of the enhancement factor and the interfacial properties", *J. Colloid Interf. Sci.*, **326**(1), 103-109. https://doi.org/10.1016/j.jcis.2008.06.052.

Chen, H.Y., Lin, M.H., Wang, C.Y., Chang, Y.M. and Gwo, S. (2015), "Large-scale hot spot engineering for quantitative SERS at the single-molecule scale", *J. Am. Chem. Soc.*, **137**(42), 13698-13705. https://doi.org/10.1021/jacs.5b09111.

Creedon, N. (2018), *Sensing at Nanostructures for Agri-Food and Enviromental Applications*, University College Cork, Ireland.

Cyrankiewicz, M., Wybranowski, T. and Kruszewski, S. (2007), "Study of SERS efficiency of metallic colloidal systems", *J. Phys.*,**79**(10), 012013. https://doi.org/10.1088/1742-6596/79/1/012013

Dehshahri, K., Nejad, M.Z., Ziaee, S., Niknejad, A. and Hadi, A. (2020), "Free vibrations analysis of arbitrary three-dimensionally FGM nanoplates", *Adv. Nano Res.*, **8**(2), 115-134. https://doi.org/10.12989/anr.2020.8.2.115.

Ding, S.Y., You, E.M., Tian, Z.Q. and Moskovits, M. (2017), "Electromagnetic theories of surface-enhanced Raman spectroscopy", *Chem. Soc. Rev.*, **46**(13), 4042-4076. https://doi.org/10.1039/C7CS00238F.

Duan, N., Chang, B., Zhang, H., Wang, Z. and Wu, S. (2016), "Salmonella typhimurium detection using a surface-enhanced Raman scattering-based aptasensor", *Int. J. Food Microbiol*, **218**, 38-43. https://doi.org/10.1016/j.ijfoodmicro.2015.11.006.

Emadi, M., Nejad, M.Z., Ziaee, S. and Hadi, A. (2021), "Buckling analysis of arbitrary two-directional functionally graded nano-plate based on nonlocal elasticity theory using generalized differential quadrature method", *Steel Compos. Struct.*, **39**(5), 565-581. https://doi.org/10.12989/scs.2022.39.5.565.

Eskandari, V. and Hadi, A. (2020), "Review of the application and mechanism of surface enhanced raman spectroscopy (sers) as biosensor for the study of biological and chemical analyzes", *J. Comput. Appl. Mech.*, **51**(2), 501-509.

Eskandari, V., Sahbafar, H., Zeinalizad, L., Marashipour, R. and Hadi, A. (2022), "A review of paper-based substrates as surface-enhanced raman spectroscopy (SERS) biosensors and microfluidic paper-based SERS platforms", *J. Comput. Appl. Mech.*, **53**(1), 132-146. https://doi.org/10.22059/jcamech.2022.322373.705.

Eskandari, V., Kordzadeh, A., Zeinalizad, L., Sahbafar, H., Aghanouri, H., Hadi, A. and Ghaderi, S. (2022), "Detection of molecular vibrations of atrazine by accumulation of silver nanoparticles on flexible glass fiber as a surface-enhanced Raman plasmonic nanosensor", *Opt. Mater.*, **128**, 112310. https://doi.org/ 10.1016/j.optmat.2022.112310.

Fan, H., Li, Y., Wu, D., Ma, H., Mao, K., Fan, D., Du, B. and Wei, Q. (2012), "Electrochemical bisphenol A sensor based on N-doped graphene sheets", *Analytica Chimica Acta*, **711**, 24-28. https://doi.org/10.1016/j.aca.2011.10.051.

Farajpour, A., Rastgoo, A. and Mohammadi, M. (2014), "Surface effects on the mechanical characteristics of microtubule networks in living cells", *Mech. Res. Commun.*, **57**, 18-26. https://doi.org/10.1016/j.mechrescom.2014.01.005.

Granger, J.H., Schlotter, N.E., Crawford, A.C. and Porter, M.D. (2016), "Prospects for point-of-care pathogen diagnostics using surface-enhanced Raman scattering (SERS)", *Chem. Soc. Rev.*, **45**(14), 3865-3882. https://doi.org/10.1039/C5CS00828J.

Hadi, A., Nejad, M.Z. and Hosseini, M. (2018a), "Vibrations of three-dimensionally graded nanobeams", *Int. J. Eng. Sci.*, **128**, 12-23. https://doi.org/10.1016/j.ijengsci.2018.03.004.

Hadi, A., Rastgoo, A., Haghighipour, N. and Bolhassani, A. (2018b), "Numerical modelling of a spheroid living cell membrane under hydrostatic pressure", *J. Stat. Mech. Theory E*, **2018**(8), 083501. https://doi.org/10.1088/1742-5468/aad369.

Hadi, A., Rastgoo, A., Bolhassani, A. and Haghighipour, N. (2019), "Effects of stretching on molecular transfer from cell membrane by forming pores", *Soft Mater.*, **17**(4), 391-399. https://doi.org/10.1080/1539445X.2019.1610974.

Iqbal, M., Usanase, G., Oulmi, K., Aberkane, F., Bendaikha, T., Fessi, H., Zine, N., Agusti, G., Errachid, E. and Elaissari, A. (2016), "Preparation of gold nanoparticles and determination of their particles size via different methods", *Mater. Res. Bull.*, **79**, 97-104. https://doi.org/10.1016/j.materresbull.2015.12.026

Jing, C. and Fang, Y. (2007), "Simple method for electrochemical preparation of silver dendrites used as active and stable SERS substrate", *J. Colloid Interf. Sci.*, **314**(1), 46-51. https://doi.org/10.1016/j.materresbull.2015.12.026

Krasteva, N., Besnard, I., Guse, B., Bauer, R.E., Müllen, K., Yasuda, A. and Vossmeyer, T. (2002), "Self-assembled gold nanoparticle/dendrimer composite films for vapor sensing applications", *Nano Lett.*, **2**(5), 551-555. https://doi.org/10.1021/nl020242s.

Le, H.H., Carlson, E.M., Chua, J.P. and Belcher, S.M. (2008), "Bisphenol A is released from polycarbonate drinking bottles

and mimics the neurotoxic actions of estrogen in developing cerebellar neurons", *Toxicol. Lett.*, **176**(2), 149-156. https://doi.org/10.1016/j.toxlet.2007.11.001.

Lee, S.N., Stolarski, V., Letton, A. and Laane, J. (2000), "Studies of bisphenol-A–polycarbonate aging by Raman difference spectroscopy", *J. Mol. Struct.*, **521**(1-3), 19-24. https://doi.org/10.1016/S0022-2860(99)00422-6.

Liang, C., Zhong, K., Liu, M., Jiang, L., Liu, S., Xing, D., . . . Tong, Y. (2010), "Synthesis of morphology-controlled silver nanostructures by electrodeposition", *Nano-Micro Lett.*, **2**(1), 6-10. https://doi.org/10.5101/nml.v2i1.p6-10.

Lucas, B.D., Kim, J.S., Chin, C. and Guo, L.J. (2008), "Nanoimprint lithography based approach for the fabrication of large-area, uniformly-oriented plasmonic arrays", *Adv. Mater.*, **20**(6), 1129-1134. https://doi.org/10.1002/adma.200700225.

Madzharova, F., Heiner, Z. and Kneipp, J. (2017), "Surface enhanced hyper-Raman scattering of the amino acids tryptophan, histidine, phenylalanine, and tyrosine", *J. Phys. Chem. C*, **121**(2), 1235-1242. https://doi.org/10.1021/acs.jpcc.6b10905.

Maragou, N.C., Makri, A., Lampi, E.N., Thomaidis, N.S. and Koupparis, M.A. (2008), "Migration of bisphenol A from polycarbonate baby bottles under real use conditions", *Food Addit. Contam.*, **25**(3), 373-383. https://doi.org/10.1080/02652030701509998.

McLellan, J.M., Li, Z.Y., Siekkinen, A.R. and Xia, Y. (2007), "The SERS activity of a supported Ag nanocube strongly depends on its orientation relative to laser polarization", *Nano Lett.*, **7**(4), 1013-1017. https://doi.org/10.1021/nl070157q.

Nerín, C., Fernández, C., Domeño, C. and Salafranca, J. (2003), "Determination of potential migrants in polycarbonate containers used for microwave ovens by high-performance liquid chromatography with ultraviolet and fluorescence detection", *J. Agric. Food Chem.*, **51**(19), 5647-5653. https://doi.org/10.1021/jf034330p.

Ngumbi, P.K., Mugo, S.W. and Ngaruiya, J.M. (2018), "Determination of gold nanoparticles sizes via surface plasmon resonance", *IOSR J Appl Chem*, **11**, 25-29. https://doi.org/10.9790/5736-1107012529.

Ntsendwana, B., Mamba, B., Sampath, S. and Arotiba, O. (2012), "Electrochemical detection of bisphenol A using graphene-modified glassy carbon electrode", *Int. J. Electrochem. Sci*, **7**(4), 3501-3512. https://doi.org/10.1007/s10800-015-0792-5.

O'Sullivan, S. (2017), "The cytotoxic and genotoxic effects of bisphenol A on neuronal cells in vitro", *Plymouth Student Scientist*, **10**(1), 41-63.

O'Reilly, A.O., Eberhardt, E., Weidner, C., Alzheimer, C., Wallace, B. and Lampert, A. (2012), "Bisphenol A binds to the local anesthetic receptor site to block the human cardiac sodium channel", *PloS one*, **7**(7), e41667. https://doi.org/10.1371/journal.pone.0041667.

Parsons, H.M., Ekman, D.R., Collette, T.W. and Viant, M.R. (2009), "Spectral relative standard deviation: A practical benchmark in metabolomics", *Analyst*, **134**(3), 478-485. https://doi.org/10.1039/B808986H.

Preethi, S., Sandhya, K., Lebonah, D.E., Prasad, C.V., Sreedevi, B., Chandrasekhar, K. and Kumari, J.P. (2014), "Toxicity of bisphenol a on humans: A review", *Int. Lett. Nat. Sci.*, **22**.

Pupo, M., Pisano, A., Lappano, R., Santolla, M.F., De Francesco, E.M., Abonante, S., Rosano, C. and Maggiolini, M. (2012), "Bisphenol A induces gene expression changes and proliferative effects through GPER in breast cancer cells and cancer-associated fibroblasts", *Environ. Health Persp.*, **120**(8), 1177-1182. https://doi.org/10.1289/ehp.1104526.

Rodriguez-Gonzalez, C., Kharissova, O.V., Martinez-Hernandez, A.L., Castano, V.M. and Velasco-Santos, C. (2013), "Graphene oxide sheets covalently grafted with keratin obtained from chicken feathers", *Digest J. Nanomater. Biostruct*, **8**(1), 127-138.

Rogers, J.A., Metz, L. and Yong, V.W. (2013), "Endocrine disrupting chemicals and immune responses: A focus on bisphenol-A and its potential mechanisms", *Mol. Immun.*, **53**(4), 421-430. https://doi.org/10.1016/j.molimm.2012.09.013

Rohani Rad, E. and Farajpour, M. R. (2019), "Dynamics analysis of microparticles in inertial microfluidics for biomedical applications", *J. Comput. Appl. Mech.*, **50**(1), 157-164.

She, G.L., Liu, H.B. and Karami, B. (2021), "Resonance analysis of composite curved microbeams reinforced with graphene nanoplatelets", *Thin Wall. Struct.*, **160**, 107407. https://doi.org/10.1016/j.tws.2020.107407.

Shrivastava, S. and Dash, D. (2010), "Label-free colorimetric estimation of proteins using nanoparticles of silver", *Nano-Micro Lett.*, **2**(3), 164-168. https://doi.org/10.5101/nml.v2i3.p164-168.

Su, S.R., Chen, Y.Y., Li, K.Y., Fang, Y.C., Wang, C.H., Yang, C.Y., Chau, L.K. and Wang, S.C. (2019), "Electrohydrodynamically enhanced drying droplets for concentration of Salmonella bacteria prior to their detections using antibody-functionalized SERS-reporter submicron beads", *Sensors Actuat. B Chem.*, **283**, 384-389. https://doi.org/10.1016/j.snb.2018.12.048.

Wang, C., Meloni, M. M., Wu, X., Zhuo, M., He, T., Wang, J., Wang, C. and Dong, P. (2019), "Magnetic plasmonic particles for SERS-based bacteria sensing: A review", *AIP Adv.*, **9**(1), 010701. https://doi.org/10.1063/1.5050858.

Wang, L.R. and Fang, Y. (2006), "IR-SERS study and theoretical analogue on the adsorption behavior of pyridine carboxylic acid on silver nanoparticles", *Spectrochim Acta Part A*, **63**(3), 614-618. https://doi.org/10.1016/j.saa.2005.06.009.

Wang, Q., Wang, Y., Liu, S., Wang, L., Gao, F., Gao, F. and Sun, W. (2012), "Voltammetric detection of bisphenol a by a chitosan–graphene composite modified carbon ionic liquid electrode", *Thin Solid Films*, **520**(13), 4459-4464. https://doi.org/10.1016/j.tsf.2012.02.069.

Wu, J., Mangham, S.C., Reddy, V., Manasreh, M. and Weaver, B. (2012), "Surface plasmon enhanced intermediate band based quantum dots solar cell", *Solar Energy Mater. Solar Cells*, **102**, 44-49. https://doi.org/10.1016/j.solmat.2012.03.032.

Yu, X., Chen, Y., Chang, L., Zhou, L., Tang, F. and Wu, X. (2013), "β-cyclodextrin non-covalently modified ionic liquid-based carbon paste electrode as a novel voltammetric sensor for specific detection of bisphenol A", *Sensor Actuat. B Chem.*, **186**, 648-656. https://doi.org/10.1016/j.snb.2013.06.089.

Yu, X., Wang, L. and Di, J. (2011), "Electrochemical deposition of high density gold nanoparticles on indium/tin oxide electrode for fabrication of biosensors", *J. Nanosci. Nanotechnol.*, **11**(12), 11084-11088. https://doi.org/10.1166/jnn.2011.3949.

Zhang, X.Y., Hu, A., Zhang, T., Lei, W., Xue, X.J., Zhou, Y. and Duley, W.W. (2011), "Self-assembly of large-scale and ultrathin silver nanoplate films with tunable plasmon resonance properties", *ACS Nano*, **5**(11), 9082-9092. https://doi.org/10.1021/nn203336m.

Zhou, H., Yang, D., Ivleva, N.P., Mircescu, N.E., Niessner, R. and Haisch, C. (2014), "SERS detection of bacteria in water by in situ coating with Ag nanoparticles", *Anal. Chem.*, **86**(3), 1525-1533. https://doi.org/10.1021/ac402935p.

JL